Research Paper
Computational Methods for Differential Equations
http://cmde.tabrizu.ac.ir
Vol. 10, No. 2, 2022, pp. 475-488
DOI:10.22034/cmde.2021.44306.1873

A Robust computational method for singularly perturbed delay parabolic convection-diffusion equations arising in the modeling of neuronal variability

Imiru Takele Daba[1,*] **and Gemechis File Dureessa**[2]

[1]Department of Mathematics, Wollega University, Nekemte, Ethiopia.

[2]Department of Mathematics, Jimma University, Jimma, Ethiopia.

Abstract

In this study, a robust computational method involving exponential cubic spline for solving singularly perturbed parabolic convection-diffusion equations arising in the modeling of neuronal variability has been presented. Some numerical examples are considered to validate the theoretical findings. The proposed scheme is shown to be an $\varepsilon-$uniformly convergent accuracy of order $O\left((\Delta t)+h^2\right)$.

Keywords. Singularly perturbed problem, Exponential cubic spline method, Implicit Euler method, Delay parabolic differential equation.
2010 Mathematics Subject Classification. 65M06, 65M70, 65M12,35B25.

1. Introduction

The motivation for considering the problem for this study lies in the mathematical model given by Stein [20], about the time evolution trajectories of the membrane potential described in terms of the families of singular perturbation problems described as [13]:

$$\frac{\partial u}{\partial t}+\frac{\sigma^2}{2}\frac{\partial^2 u}{\partial x^2}+\left(\mu_D-\frac{x}{\tau}\right)\frac{\partial u}{\partial x}+\lambda_s u(x+a_s,t)+\omega_s u(x+i_s,t)-(\lambda_s+\omega_s)u(x,t)=0, \tag{1.1}$$

where the reaction terms are correspond to the superposition of excitatory and inhibitory inputs.

Because of the structure of the model (1.1), one can hardly obtain its exact solution. Therefore, to study the behavior of this model, it is very important to devise efficient numerical methods that provide more accurate solutions to the problem.

Various scholars tried to develop numerical methods for solving singularly perturbed delay parabolic partial differential equations (SPDPPDEs) with shift arguments in the space variable of the type (1.1) and analyzing the effects of shift parameters on the solution profile, [10, 11, 15, 16, 22] are some to mention. The methods in [11, 15, 16] were developed an adaptive Shishkin mesh discretization type method to resolve the layer, but requires **a priori** knowledge of the position and width of the boundary layer of the problem. This requires experience and in depth insight about the problem which may be difficult for the beginners to understand.

Further, authors [2, 3] developed numerical methods that are applicable for the general arguments where the delay and advance parameters are both smaller, $o(\varepsilon)$ and greater, $O(\varepsilon)$ than the perturbation parameter for the problem of the type (1.1). However, their convergence is not independent of the perturbation parameter that highly affects the solution profile of the family of the problems under consideration.

More recently, Bullo *et al.* [9], suggested an $\varepsilon-$uniform numerical method to solve singularly perturbed parabolic reaction-diffusion problem using fitted operator technique. Nowadays, non-polynomial spline methods have gained

Received: 30 January 2021 ; Accepted: 01 May 2021.
∗ Corresponding author. Email: imirutakele@gmail.com.

popularity as a powerful technique to solve partial differential equations. For instance, Zadvan and Rashidinia [23], developed a collocation method using TS B-spline functions to solve the nonlinear Klein-Gordon equation.

Further, numerical treatment of families of the problem under consideration using most contemporary numerical methods on a uniform step size could not capture the solution in the layer region of the solution and hence such numerical methods are unstable [18]. To overcome this limitation, the layer adaptive meshes have been developed by Bakhvalov [1], Shishkin [19], and others, but they require a priori knowledge of the location and breadth of the boundary layer(s) that in turn increase the difficulty of finding the solution of the problem under consideration.

Hence, the objective of this study is to develop a numerical method that does not require a priori information about the location and width of the boundary layer, parameter uniform convergent and requires less computational effort to solve the families of the problem under consideration that arises in the modeling of neuronal variability. The formulation of the method and its corresponding error analysis are treated in the subsequent sections.

2. Continuous Problem

In this paper, we consider the following model problem on the domain $D = \Omega_x \times \Omega_t = (0,1) \times (0,T]$:

$$\begin{cases} \frac{\partial u}{\partial t} - \varepsilon^2 \frac{\partial^2 u}{\partial x^2} + \xi(x)\frac{\partial u}{\partial x} + \nu(x)u(x-\delta,t) + \varrho(x)u(x,t) = \eta(x,t), \\ (x,t) \in D, u(x,0) = u_0(x), x \in D_0 = \{(x,0) : x \in \overline{\Omega}_x\}, \\ u(x,t) = \Upsilon_1(x,t), \forall (x,t) \in D_L = \left\{(x,t) : -\delta \le x \le 0, t \in \overline{\Omega}_t\right\}, \\ u(1,t) = \Upsilon_2(1,t), \forall t \in \overline{\Omega}_t, \end{cases} \tag{2.1}$$

where $0 < \varepsilon \ll 1$ is a singular perturbation parameter and δ is a delay parameter of $o(\varepsilon)$. The functions $\xi(x), \nu(x), \varrho(x)$, $\eta(x,t), \Upsilon_1(x,t), \Upsilon_2(1,t)$ and $u_0(x)$ are considered to be sufficiently smooth, bounded and independent of ε. We also considered $\nu(x) + \varrho(x) \ge \zeta > 0 \ \ \forall x \in \overline{\Omega}_x$, for some positive constant ζ.

When $\delta < \varepsilon$, the use of Taylor's series expansion for the terms containing shift arguments is valid [21]. Consequently, we considered this case, and applying Taylor's series expansion, we get

$$u(x-\delta,t) \approx u(x,t) - \delta\frac{\partial u(x,t)}{\partial x} + \frac{\delta^2}{2}\frac{\partial^2 u(x,t)}{\partial x^2} + O(\delta^3). \tag{2.2}$$

Substituting Eq. (2.2) into Eq. (2.1), we obtain:

$$\begin{cases} L_\varepsilon u(x,t) = r(x)\frac{\partial u(x,t)}{\partial t} - \varepsilon\frac{\partial^2 u(x,t)}{\partial x^2} + \theta(x)\frac{\partial u(x,t)}{\partial x} + \vartheta(x)u(x,t) = \gamma(x,t), \\ u(x,0) = u_0(x), x \in \overline{\Omega}_x, \\ u(0,t) = \Upsilon_1(0,t), t \in \overline{\Omega}_t, \\ u(1,t) = \Upsilon_2(1,t), t \in \overline{\Omega}_t, \end{cases} \tag{2.3}$$

where

$$r(x) = \frac{1}{\left(\varepsilon - \left(\frac{\delta^2}{2\varepsilon}\right)\xi(x)\right)}, \quad \theta(x) = \left(\frac{\xi(x) - \delta\nu(x)}{\varepsilon - \left(\frac{\delta^2}{2\varepsilon}\right)\nu(x)}\right),$$
$$\vartheta(x) = \left(\frac{\nu(x)+\varrho(x)}{\varepsilon - \left(\frac{\delta^2}{2\varepsilon}\right)\xi(x)}\right), \gamma(x,t) = \left(\frac{\eta(x,t)}{\varepsilon - \left(\frac{\delta^2}{2\varepsilon}\right)\xi(x)}\right).$$

For small δ, Eq. (2.1) and Eq. (2.3) have an almost equal approximate solution. We assume that $0 < r(x) \le 1/\left(\varepsilon - \left(\frac{\delta^2}{\varepsilon}\right)K\right) = r$, where, $\xi(x) \ge 2K$. It is also assumed that $\theta(x) \ge \theta^* > 0, \ \forall \ x \in \overline{\Omega}_x$ and some constant θ^*, which implies that the boundary layer occurs near $x = 1$. If $\theta(x) \le \theta^* < 0, \ \forall \ x \in \overline{\Omega}_x$, then the boundary layer will occur near $x = 0$. Moreover, it is assumed that $\vartheta(x) \ge \vartheta^* > 0, \ \forall x \in \overline{\Omega}$ for some constant ϑ^*.

To elude conflict between boundary and initial condition, we assume the compatibility conditions on the corner of the domain $(0,0)$ and $(0,1)$ as [12]

$$u_0(0) = \Upsilon_1(0,0), \quad u_0(1) = \Upsilon_2(1,0),$$

and

$$\begin{cases} r(0)\frac{\partial \Upsilon_1 i(0,0)}{\partial t} - \varepsilon\frac{\partial^2 u_0(0)}{\partial x^2} + \theta(0)\frac{\partial u_0(0)}{\partial x} + \vartheta(0)u_0(0) = \gamma(0,0), \\ r(1)\frac{\partial \Upsilon_2(1,0)}{\partial t} - \varepsilon\frac{\partial^2 u_0(1)}{\partial x^2} + \theta(1)\frac{\partial u_0(1)}{\partial x} + \vartheta(1)u_0(1) = \gamma(1,0). \end{cases}$$

Lemma 2.1. *(Maximum principle). Let $\Xi(x,t) \in C^{2,1}\overline{D}$. If $\Xi(x,t) \geq 0, \forall (x,t) \in \partial D$ $(\partial D = \overline{D} - D)$ and $L_\varepsilon \Xi(x,t) \geq 0, \forall (x,t) \in D$, then $\Xi(x,t) \geq 0, \forall (x,t) \in \overline{D}$.*

Proof Let $(\hat{x},\hat{t}) \in \overline{D}$ be such that

$$\Xi(\hat{x},\hat{t}) = \min_{(x,t)\in\overline{D}} \Xi(x,t) < 0. \tag{2.4}$$

Then, we have $(\hat{x},\hat{t}) \notin \partial D$, and $\Xi_x(\hat{x},\hat{t}) = 0, \Xi_t(\hat{x},\hat{t}) = 0$, $\Xi_{xx}(\hat{x},\hat{t}) \geq 0$. Now,

$$L_\varepsilon \Xi(\hat{x},\hat{t}) = r(x)\frac{\partial \Xi(\hat{x},\hat{t})}{\partial t} - \varepsilon\frac{\partial^2 \Xi(\hat{x},\hat{t})}{\partial x^2} + \theta(x)\frac{\partial \Xi(\hat{x},\hat{t})}{\partial x} + \vartheta(x)\Xi(\hat{x},\hat{t}) < 0,$$

that contradicts the assumption made above. It follows that $\Xi(\hat{x},\hat{t}) \geq 0$ and hence $\Xi(x,t) \geq 0, \forall (x,t) \in \overline{D}$. □

Lemma 2.2. *The solution $u(x,t)$ of Eq. (2.3) satisfies*

$$\|u\| \leq (\vartheta^*)^{-1} \|\gamma\| + \max\left\{|u_0(x)|, \max\left\{|\Upsilon_1(0,t)|, |\Upsilon_2(1,t)|\right\}\right\},$$

where, $\|.\|$ is the L_∞ norm given by $\|u\| = \max_{(x,t)\in\overline{D}} |u(x,t)|$.

Proof Let $\Xi^{\pm}(x,t)$ be two barrier functions defined by

$$\Xi^{\pm}(x,t) = (\vartheta^*)^{-1} \|\gamma\| + \max\left\{|u_0(x)|, \max\left\{|\Upsilon_1(0,t)|, |\Upsilon_2(1,t)|\right\}\right\} \pm u(x,t).$$

Then at the initial value and the two end points, we have

$$\Xi^{\pm}(x,0) = (\vartheta^*)^{-1} \|\gamma\| + \max\left\{|u_0(x)|, \max\left\{|\Upsilon_1(0,0)|, |\Upsilon_2(1,0)|\right\}\right\} \pm u(x,0) \geq 0,$$
$$\Xi^{\pm}(0,t) = (\vartheta^*)^{-1} \|\gamma\| + \max\left\{|u_0(0)|, \max\left\{|\Upsilon_1(0,t)|, |\Upsilon_2(1,t)|\right\}\right\} \pm u(0,t) \geq 0,$$
$$\Xi^{\pm}(1,t) = (\vartheta^*)^{-1} \|\gamma\| + \max\left\{|u_0(1)|, \max\left\{|\Upsilon_1(0,t)|, |\Upsilon_2(1,t)|\right\}\right\} \pm u(1,t) \geq 0.$$

Using L_ε operator in Eq. (2.3) on $\Xi^{\pm}(x,t)$ we have

$$\begin{aligned} L_\varepsilon \Xi^{\pm}(x,t) &= r(x)\frac{\partial \Xi^{\pm}(x,t)}{\partial t} - \varepsilon\frac{\partial^2 \Xi^{\pm}(x,t)}{\partial x^2} + \theta(x)\frac{\partial \Xi^{\pm}(x,t)}{\partial x} + \vartheta(x)\Xi^{\pm}(x,t) \\ &= \vartheta(x)\left((\vartheta^*)^{-1} \|\gamma\| + \max\left\{|u_0(x)|, \max\left\{|\Upsilon_1(0,t)|, |\Upsilon_2(1,t)|\right\}\right\}\right) \pm L_\varepsilon u(x,t), \\ &\geq \vartheta(x)\left((\vartheta^*)^{-1} \|\gamma\| + \max\left\{|u_0(x)|, \max\left\{|\Upsilon_1(0,t)|, |\Upsilon_2(1,t)|\right\}\right\}\right) \pm \gamma(x,t) \\ &\geq \vartheta(x)\left(\max\left\{|u_0(x)|, \max\left\{|\Upsilon_1(0,t)|, |\Upsilon_2(1,t)|\right\}\right\}\right) + \vartheta(x)(\vartheta^*)^{-1} \|\gamma\| \pm \gamma(x,t). \end{aligned}$$

Using the fact $\vartheta(x) \geq \vartheta^* > 0$, we have $\vartheta(x)(\vartheta^*)^{-1} \geq 1$ and substituting it in the above inequality, we obtain

$$L_\varepsilon \Xi^{\pm}(x,t) \geq 0, , \quad \forall (x,t) \in \overline{D}, \text{ since } \|\gamma\| \geq \gamma(x,t).$$

This implies that $L_\varepsilon \Xi^{\pm}(x,t) \geq 0$. Hence by Lemma (2.1) we have, $\Xi^{\pm}(x,t) \geq 0$, $\forall (x,t) \in \overline{D}$, which gives

$$\|u\| \leq (\vartheta^*)^{-1} \|\gamma\| \max\left\{|u_0(x)|, \max\left\{|\Upsilon_1(0,t)|, |\Upsilon_2(1,t)|\right\}\right\}.$$

□

3. Formulation of the numerical scheme

To formulate the numerical scheme, we first discretize the temporal variable using the implicit Euler scheme (*i.e.,* theta-scheme $\theta = 1$) on a uniform mesh.

3.1. **Temporal discretization.** So far, the construction of $\theta-$scheme for the time variable discretization in problems consisting of PDEs has been popular. See for instance, [4–8] and references therein. We divide the time domain $[0,T]$ into M equidistant mesh with time step size Δt such that

$$D^M = \left\{ (x,t_j) : x \in \Omega_x, t_j = j\Delta t = j\left(\frac{T}{M}\right),\ \forall\, 0 \le j \le M \right\}.$$

Applying the implicit Euler scheme on t, yields

$$\begin{cases} L_\varepsilon^M U^{j+1}(x) = \nu^{j+1}(x), \\ U(x,0) = U_0(x), \quad x \in \overline{\Omega}_x, \\ U^{j+1}(0) = \Upsilon_1^{j+1}(0) \quad \forall\, 0 \le j+1 < M, \\ U^{j+1}(1) = \Upsilon_2^{j+1}(1) \quad \forall\, 0 \le j+1 < M, \end{cases} \tag{3.1}$$

where, $L_\varepsilon^M U^{j+1}(x) = -\varepsilon \frac{\partial^2 U^{j+1}(x)}{\partial x^2} + \theta(x)\frac{\partial U^{j+1}(x)}{\partial x} + s(x)U^{j+1}(x)$,
$s(x) = \left(\frac{r(x)}{\Delta t} + \vartheta(x)\right)$, $\nu^{j+1}(x) = \left(\gamma^{j+1}(x) + \frac{r(x)U^j(x)}{\Delta t}\right)$.

Lemma 3.1. *(Discrete maximum principle). Let $\Xi(x) \in C^2(\overline{\Omega}_x)$. If $\Xi^{j+1}(0) \ge 0$, $\Xi^{j+1}(1) \ge 0$, and $L_\varepsilon^M \Xi^{j+1}(x) \ge 0, \forall (x) \in \Omega_x$, then $\Xi^{j+1}(x) \ge 0, \forall (x) \in \overline{\Omega}_x$.*

Proof The proof can easily be derived by using a similar argument as used in Lemma 2.1 □

Lemma 3.2. *[Local error estimate(LEE)]. If $\left|\frac{\partial^k u(x,t)}{\partial t^k}\right| \le C,\ \forall\,(x,t) \in \overline{D}, k = 0,1,2$, then the LEE $e_{j+1} = u(x,t_{j+1}) - U^{j+1}(x)$ in the temporal direction at $(j+1)$ th time level satisfies*

$$\|e_{j+1}\| \le C\,(\Delta t)^2.$$

Proof The detailed proof of this lemma is given in [3]. □

Lemma 3.3. *[Global error estimate]. Under the hypothesis of Lemma 3.2, the global error estimate (E_j) in the temporal direction at (j)th time level satisfies*

$$\|E_j\|_\infty \le C(\Delta t),\ \forall\ j \le T/\Delta t,$$

Proof Using LEE up to jth time step given in Lemma 3.3, we have

$$\begin{aligned} \|E_j\|_\infty &= \left\| \sum_{i=1}^{j} e_i \right\|_\infty,\ j \le T/\Delta t, \\ &\le \|e_1\|_\infty + \|e_2\|_\infty + \|e_3\|_\infty + \cdots + \|e_j\|_\infty \\ &\le c_1 j\,(\Delta t)^2, \quad \text{by Lemma 3.2}, \\ &\le c_1\,(j\Delta t)\,\Delta t, \\ &\le c_1 T\,(\Delta t), \quad (j\Delta t \le T) \\ &\le C\,(\Delta t), \end{aligned}$$

where C is a positive constant independent of ε and Δt. □

3.2. **Spatial discretization.** We divide the space domain $[0,1]$ into N equidistant mesh with spatial step size h such that

$$D^N = \{x_i = ih, \forall i = 1,2,3,\cdots,N, x_0 = 0, x_N = 1, h = 1/N\}.$$

Let us rewrite Eq. (3.1) for $x \in \Omega_x, j = 0,1\cdots,M-1$ as

$$-\varepsilon\frac{\partial^2 U^{j+1}(x)}{\partial x^2} + \theta(x)\frac{\partial U^{j+1}(x)}{\partial x} + s(x)U^{j+1}(x) = \nu^{j+1}(x), \tag{3.2}$$

subject to the boundary conditions

$$U^{j+1}(0) = \Upsilon_1^{j+1}(0), \quad \text{and} \quad U^{j+1}(1) = \Upsilon_2^{j+1}(1). \tag{3.3}$$

Now, we use an exponential cubic spline method to find the approximate solution of Eqs. (3.2) and (3.3) on a uniform step size as follows. Let U_i^{j+1} be an approximation to the exact solution $U^{j+1}(x_i)$ of Eqs. (3.2) and (3.3) obtained by the segment $E_\triangle(x)$ passing through the points $\left(x_i, U_i^{j+1}\right)$ and $\left(x_{i+1}, U_{i+1}^{j+1}\right)$. Each mixed spline segment $E_\triangle^{j+1}(x)$ has the form [24]:

$$E_\triangle^{j+1}(x) = a_i e^{k(x-x_i)} + b_i e^{-k(x-x_i)} + c_i(x-x_i) + d_i, i = 0, 1, 2, \cdots, N, \tag{3.4}$$

where, a_i, b_i, c_i, and d_i are constants and $k \neq 0$ is a free parameter that will be used to raise the accuracy of the method. To find the unknown coefficients in Eq. (3.4), let us denote:

$$\begin{aligned} &E_\triangle^{j+1}(x_i) = U_i^{j+1}, && E_\triangle^{j+1}(x_{i+1}) = U_{i+1}^{j+1}, \\ &\frac{\partial^2 E_\triangle^{j+1}(x_i)}{\partial x^2} = M_i, && \frac{\partial^2 E_\triangle^{j+1}(x_{i+1})}{\partial x^2} = M_{i+1}. \end{aligned} \tag{3.5}$$

Straightforward manipulations yields:

$$\begin{aligned} &a_i = \frac{h^2\left(M_{i+1} - M_i e^{-\theta}\right)}{2\theta^2 \sinh(\theta)}, && b_i = \frac{h^2\left(M_i e^{\theta} - M_{i+1}\right)}{2\theta^2 \sinh(\theta)}. \\ &c_i = \frac{\left(U_{i+1}^{j+1} - U_i^{j+1}\right)}{h} - \frac{h(M_{i+1} - M_i)}{\theta^2}, && d_i = U_i^{j+1} - \left(\frac{h^2}{\theta^2} M_i\right) \end{aligned} \tag{3.6}$$

Using the continuity condition of the first derivative at $x = x_i$, that is $E_{\triangle-1}(x_i) = E_\triangle(x_i)$, we obtain

$$h^2\left(\alpha M_{i-1} + 2\beta M_i + \alpha M_{i+1}\right) = \left(U_{i-1}^{j+1} - 2U_i^{j+1} + U_{i+1}^{j+1}\right), i = 1, 2, \cdots, N-1, \tag{3.7}$$

where

$$\alpha = \left(\frac{\sinh(\theta) - \theta}{\theta^2 \sinh(\theta)}\right) \quad and \quad \beta = \left(\frac{2\theta\cosh(\theta) - 2\sinh(\theta)}{\theta^2 \sinh(\theta)}\right)$$

Equation (3.2) at $x = x_k$ can be written as:

$$-\varepsilon M_k + \theta_k \frac{\partial U^{j+1}(x_k)}{\partial x} + s_k U^{j+1}(x_k) = \nu_k^{j+1}, , k = i, i \pm 1, \tag{3.8}$$

where we approximate $\frac{\partial U^{j+1}(x_k)}{\partial x}$ as:

$$\begin{aligned} &\frac{\partial U^{j+1}(x_{i-1})}{\partial x} \approx \frac{-U_{i+1}^{j+1} + 4U_i^{j+1} - 3U_{i-1}^{j+1}}{2h}, \\ &\frac{\partial U^{j+1}(x_i)}{\partial x} \approx \frac{U_{i+1}^{j+1} - U_{i-1}^{j+1}}{2h}, \\ &\frac{\partial U^{j+1}(x_{i+1})}{\partial x} \approx \frac{3U_{i+1}^{j+1} - 4U_i^{j+1} + U_{i-1}^{j+1}}{2h}. \end{aligned} \tag{3.9}$$

Substituting Eqs. (3.8) and (3.9) into Eq. (3.7) and introducing a fitting factor $\sigma(\rho)$, which is used to handle the effect of the singular perturbation on solution behavior, into the resulting equation gives

$$\begin{aligned} &\left(\frac{-\sigma(\rho)}{\rho} - \frac{3\alpha\theta_{i-1}}{2} - \beta\theta_i + \frac{\alpha\theta_{i+1}}{2} + h\alpha s_{i-1}\right)U_{i-1}^{j+1} + \left(\frac{2\sigma(\rho)}{\rho} + 2\alpha\theta_{i-1} - 2\alpha\theta_{i+1} + 2h\beta s_i\right)U_i^{j+1} \\ &\quad + \left(\frac{-\sigma(\rho)}{\rho} - \frac{\alpha\theta_{i-1}}{2} + \beta\theta_i + \frac{3\theta_{i+1}}{2} + h\alpha s_{i+1}\right)U_{i+1}^{j+1} \\ &\quad = h\left(\alpha\nu_{i-1}^{j+1} + \beta\nu_i^{j+1} + \alpha\nu_{i+1}^{j+1}\right), \end{aligned} \tag{3.10}$$

where $\rho = \frac{h}{\varepsilon}$.

Taking the limit of Eq. (3.10) as $h \to 0$:

$$\begin{aligned} &\lim_{h\to 0}\left(\frac{\sigma(\rho)}{\rho}\right)\left(U^{j+1}(ih-h) - 2U^{j+1}(ih) + U^{j+1}(ih+h)\right) + \\ &(\alpha+\beta)\lim_{h\to 0}\left(\theta(ih)\right)\left(U^{j+1}(ih+h) - U^{j+1}(ih-h)\right) = 0. \end{aligned} \tag{3.11}$$

For problems with a layer at the right end of the interval, using the theory of singular perturbations, the solution of Eqs. (3.2) and (3.3) takes the form [14]

$$U^{j+1}(x) \approx U_o^{j+1}(x) + \frac{\theta(1)}{\theta(x)}(\Upsilon_2^{j+1}(1) - U_0^{j+1}(1)) \exp\left(-\theta(x)\frac{(1-x)}{\varepsilon}\right) + O(\varepsilon), \tag{3.12}$$

where $U_0^{j+1}(x)$ is the solution of the reduced problem

$$\theta(x)\frac{\partial U_0^{j+1}(x)}{\partial x} + s(x)U_0^{j+1}(x) = \nu^{j+1}(x), \text{ with } U_0^{j+1}(1) = \Upsilon_2^{j+1}(1).$$

Taking Taylor's series expansion for $\theta(x)$ about the point $x = 1$ and restricting to their first terms, Eq. (3.12) becomes

$$U^{j+1}(x) \approx U_o^{j+1}(x) + (\Upsilon_2^{j+1} - U_0^{j+1}(1)) \exp\left(-\theta(1)\frac{(1-x)}{\varepsilon}\right) + O(\varepsilon). \tag{3.13}$$

Equation (3.13) at $x_i = ih$ and as $h \to 0$ becomes

$$\lim_{h\to 0} U^{j+1}(ih) \approx U_o^{j+1}(ih) + (\Upsilon_2^{j+1} - U_0^{j+1}(1)) \exp\left(-\theta(1)\left(\frac{1}{\varepsilon} - i\rho\right)\right) + O(\varepsilon). \tag{3.14}$$

Plugging Eq. (3.13) into Eq. (3.10), we obtain the required fitting factor

$$\sigma(\rho) = \theta(0)(\alpha+\beta)\coth\left(\frac{\theta(1)\rho}{2}\right), \tag{3.15}$$

Equation (3.10) can be written as:

$$A_i U_{i-1}^{j+1} - B_i U_i^{j+1} + C_i U_{i+1}^{j+1} = F_i, \text{ for } i = 1, 2, \cdots, N-1, \tag{3.16}$$

where

$$\begin{aligned}
A_i &= \tfrac{-\sigma(\rho)}{\rho} - \tfrac{3\alpha\theta_{i-1}}{2} - \beta\theta_i + \tfrac{\alpha\theta_{i+1}}{2} + h\alpha s_{i-1},\\
B_i &= \tfrac{-2\sigma(\rho)}{\rho} - 2\alpha\theta_{i-1} - 2\alpha\theta_{i+1} + 2h\beta s_i,\\
C_i &= \tfrac{-\sigma(\rho)}{\rho} - \tfrac{\alpha\theta_{i-1}}{2} + \beta\theta_i + \tfrac{3\theta_{i+1}}{2} + \alpha h s_{i+1},\\
F_i &= h\left(\alpha\nu_{i-1}^{j+1} + 2\beta\nu_i^{j+1} + \alpha\nu_{i+1}^{j+1}\right).
\end{aligned}$$

4. Error analysis

Lemma 4.1. *The solution of the semi-discrete problem (3.2) satisfies the bound*

$$\left|U^{j+1}(x_i) - U_i^{j+1}\right| \le Ch^2,$$

where C is a constant independent of ε and h.

Proof From the approximations given in Eq. (3.9) we have

$$\begin{aligned}
e_i' &= \frac{\partial U^{j+1}(x_i)}{\partial x} - \frac{\partial U_i^{j+1}}{\partial x} = -\frac{h^2}{6}\frac{\partial^3 U^{j+1}(x_i)}{\partial x^3} - \frac{h^4}{120}\frac{\partial^5 U^{j+1}(\chi_i)}{\partial x^5},\\
e_{i+1}' &= \frac{\partial U^{j+1}(x_{i+1})}{\partial x} - \frac{\partial U_{i+1}^{j+1}}{\partial x} = \frac{h^2}{3}\frac{\partial^3 U^{j+1}(x_i)}{\partial x^3} + \frac{h^3}{12}\frac{\partial^4 U^{j+1}(x_i)}{\partial x^4} + \frac{h^4}{30}\frac{\partial^5 U^{j+1}(\chi_i)}{\partial x^5},\\
e_{i-1}' &= \frac{\partial U^{j+1}(x_{i-1})}{\partial x} - \frac{\partial U_{i-1}^{j+1}}{\partial x} = \frac{h^2}{3}\frac{\partial^3 U^{j+1}(x_i)}{\partial x^3} - \frac{h^3}{12}\frac{\partial^4 U^{j+1}(x_i)}{\partial x^4} + \frac{h^4}{30}\frac{\partial^5 U^{j+1}(\chi_i)}{\partial x^5},
\end{aligned} \tag{4.1}$$

where $x_{i-1} < \chi < x_{i+1}$.
Now, using $\sigma\varepsilon M_k = \theta_k \frac{\partial U_k^{j+1}}{\partial x} + s_k U_k^{j+1} - \nu_k^{j+1}$, $k = i, i \pm 1$, in Eq. (3.7) gives

$$\sigma(\rho)\varepsilon\left(U_{i-1}^{j+1} - 2U_i^{j+1} + U_{i+1}^{j+1}\right) = h^2\alpha\left(\theta_{i-1}\frac{\partial U_{i-1}^{j+1}}{\partial x} + s_{i-1}U_{i-1} - \nu_{i-1}\right) + 2h^2\beta\left(\theta_i\frac{\partial U_i^{j+1}}{\partial x} + s_i U_i^{j+1} - \nu_i^{j+1}\right) + h^2\alpha\left(\theta_{i+1}\frac{\partial U_{i+1}^{j+1}}{\partial x} + s_{i+1}U_{i+1}^{j+1} - \nu_{i+1}^{j+1}\right). \tag{4.2}$$

Considering the corresponding exact solution to Eq. (4.2) we have

$$\begin{aligned}\sigma(\rho)\varepsilon\left(U^{j+1}(x_{i-1}) - 2U^{j+1}(x_i) + U(x_{i+1})\right) &= h^2\alpha\theta(x_{i-1})\frac{\partial U^{j+1}(x_{i-1})}{\partial x} + h^2\alpha\Big(s(x_{i-1})U^{j+1}(x_{i-1}) \\ &\quad - \nu^{j+1}(x_{i-1})\Big) \\ &\quad + 2h^2\beta\left(\theta(x_i)\frac{\partial U^{j+1}(x_i)}{\partial x} + s(x_i)U^{j+1}(x_i)\right) \\ &\quad - 2h^2\beta\left(\nu^{j+1}(x_i)\right) \\ &\quad + h^2\alpha\left(\theta(x_{i+1})\frac{\partial U^{j+1}(x_{i+1})}{\partial x} + s(x_{i+1})U^{j+1}(x_{i+1}) - \nu^{j+1}(x_{i+1})\right).\end{aligned} \tag{4.3}$$

Subtracting Eq. (4.2) from Eq. (4.3) and substituting $e_k = U^{j+1}(x_k) - U_k^{j+1}$, for $k = i, i \pm 1$ we arrive at

$$\begin{aligned}\left(\sigma(\rho)\varepsilon - h^2\alpha s_{i-1}\right)e_{i-1} + \left(-2\sigma(\rho)\varepsilon - 2h^2\beta s_i\right)e_i + \left(\sigma(\rho)\varepsilon - h^2\alpha s_{i+1}\right)e_{i+1} \\ = h^2\left(\alpha\theta_{i-1}e_{i-1}^{'} + 2\beta\theta_i e_i^{'} + \alpha\theta_{i+1}e_{i+1}^{'}\right).\end{aligned} \tag{4.4}$$

Using Eq. (4.1) into Eq. (4.4), we obtain

$$\begin{aligned}\left(\sigma(\rho)\varepsilon - h^2\alpha s_{i-1}\right)e_{i-1} + \left(-2\sigma(\rho)\varepsilon - 2h^2\beta s_i\right)e_i + \left(\sigma(\rho)\varepsilon - h^2\alpha s_{i+1}\right)e_{i+1} \\ = \frac{h^4}{3}\left(\alpha\theta_{i-1} - \beta\theta_i + \alpha\theta_{i+1}\right)U^{(3)}(x_i) + \frac{h^5}{12}\left(-\alpha\theta_{i-1} + \alpha\theta_{i+1}\right)U^{(4)}(x_i) \\ + \frac{h^6}{60}\left(2\alpha\theta_{i-1} - \beta\theta_i + 2\alpha\theta_{i+1}\right)U^{(5)}(\chi_i).\end{aligned} \tag{4.5}$$

Using the expressions $\theta_{i-1} = \theta_i - h\theta_i' + \frac{h^2}{2!}\theta^{(2)}(\chi_i)$ and $\theta_{i+1} = \theta_i + h\theta_i' + \frac{h^2}{2!}\theta^{(2)}(\chi_i)$ in Eq. (4.5) provides

$$\left(\sigma(\rho)\varepsilon - h^2\alpha s_{i-1}\right)e_{i-1} + \left(-2\sigma(\rho)\varepsilon - 2h^2\beta s_i\right)e_i + \left(\sigma(\rho)\varepsilon - h^2\alpha s_{i+1}\right)e_{i+1} = T_i(h), \tag{4.6}$$

where $T_i(h) = \frac{h^4}{3}(2\alpha - \beta)\theta_i U^{(3)}(x_i) + O(h^6)$. Therefore, $T_i(h) = O\left(h^4\right)$ for the choice of parameters $\alpha + \beta = 1/2$. The matrix representation of Eq. (4.6) is

$$(D - M)\tau = \hat{T}, \tag{4.7}$$

where
$D = trid\left(-\sigma(\rho)\varepsilon, 2\sigma(\rho)\varepsilon, -\sigma(\rho)\varepsilon\right)$, $M = trid\left(h^2\alpha s_{i-1}, 2h^2\alpha s_i, h^2\alpha s_{i+1}\right)$,
$\tau = [e_1, e_2, \cdots, e_{N-1}]^T$ and $\hat{T} = [-T_1(h), -T_2(h), \cdots, -T_{N-1}(h)]^T$. Following [17], it can be shown that

$$\|\tau\| \leq \frac{C}{h^2} \times O\left(h^4\right) = Ch^2, \tag{4.8}$$

where C is a constant, independent of h and ε. □

Lemma 4.2. *Let $u(x_i, t_{j+1})$ be the solution of problem (2.3) at each grid point (x_i, t_{j+1}) and U_i^{j+1} be its approximate solution obtained by the proposed scheme given in Eq. (3.16). Then, the error estimate for the fully discrete scheme is given by*

$$\left|u(x_i, t_{j+1}) - U_i^{j+1}\right| \leq C\left((\Delta t) + h^2\right).$$

Proof Combining Lemma 3.3 and Lemma 4.1, we get the required estimate. □

5. Numerical examples and illustrations

Two examples are presented to testify the theoretical findings. In all cases, we performed numerical experiments by taking $\alpha = 1e-04$ and $\beta = 4.999e-01$. As the exact solutions of these examples are not known, the maximum pointwise error for the given examples is computed by using the double mesh principle given in [22]:

$$E_{\varepsilon,\delta}^{N,M} = \max_{1\leq i,j\leq N-1, M-1} \left|U_{i,j}^{N,M} - U_{i,j}^{2N,2M}\right|,$$

where $U_{i,j}^{N,M}$ are computed numerical solutions obtained on the mesh $D^{N,M} = \Omega_x^N \times \Omega_t^M$ and $U_{i,j}^{2N,2M}$ are computed numerical solutions on the mesh $D^{2N,2M} = \Omega_x^{2N} \times \Omega_t^{2M}$ with N and M mesh intervals in the spatial and temporal directions respectively.

The $\varepsilon-$uniform errors $(E^{N,M})$, order of convergence $\left(\Gamma_{\varepsilon,\delta}^{N,M}\right)$ and $\varepsilon-$uniform order of convergence $\left(\Gamma^{N,M}\right)$ is calculated using

$$E^{N,M} = \max_{\varepsilon,\delta}\left\{E_{\varepsilon,\delta}^{N,M}\right\}, \Gamma_{\varepsilon,\delta}^{N,M} = \log_2\left(\frac{E_{\varepsilon,\delta}^{N,M}}{E_{\varepsilon,\delta}^{2N,2M}}\right) \text{ and } \Gamma^{N,M} = \log_2\left(\frac{E^{N,M}}{E^{2N,2M}}\right)$$

respectively.

Example 5.1. [11]. Consider a SPDPPDEs of the form in (2.1)

$$\begin{cases} \frac{\partial u}{\partial t} - \varepsilon^2 \frac{\partial^2 u}{\partial x^2} + \left(2 + x + x^2\right)\frac{\partial u}{\partial x} + \left(\frac{1+x^2}{2}\right)u(x-\delta, t) = \sin(\pi x(1-x)), \\ u_0(x) = 0, u(x,t) = 0, \forall (x,t) \quad \exists D_L = \{(x,t) : -\delta \leq x \leq 0, 0 \leq t \leq 1\}, u(1,t) = 0, \quad 0 \leq t \leq 1, T = 1. \end{cases}$$

Example 5.2. [15]. Consider a SPDPPDEs of the form in (2.1)

$$\begin{cases} \frac{\partial u}{\partial t} - \varepsilon^2 \frac{\partial^2 u}{\partial x^2} + (2 + x + x^2)\frac{\partial u}{\partial x} + (\frac{1+x^2}{2})u(x-\delta, t) = \sin(\pi x(1-x))t, \\ u_0(x) = 0, \forall (x,t) \quad \exists D_L = \{(x,t) : -\delta \leq x \leq 0, 0 \leq t \leq 1\}, u(1,t) = 0, \quad 0 \leq t \leq 1, T = 1. \end{cases}$$

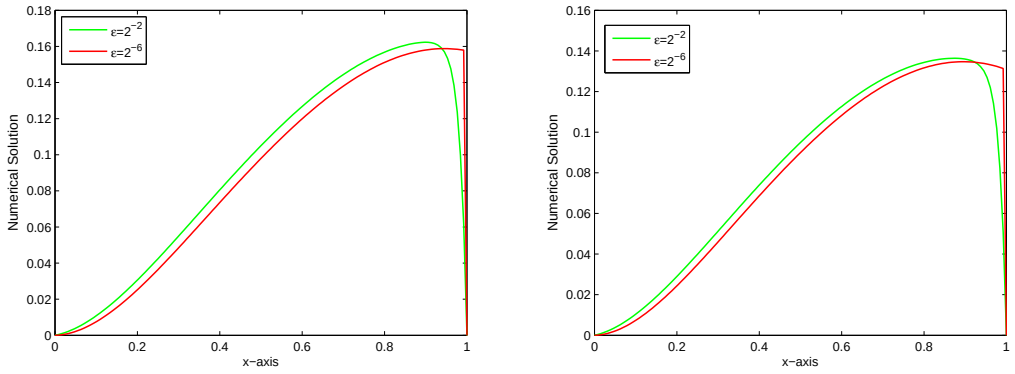

(A) Example 5.1 (B) Example 5.2

Figure 1. The solution behavior for different values of ε at $T = 1, \delta = 0.5 \times \varepsilon$, and $N = M = 128$.

TABLE 1. $E^{N,M}_{\varepsilon,\delta}$, $E^{N,M}, \Gamma^{N,M}_{\varepsilon,\delta}$ and $\Gamma^{N,M}$ for Example 5.1 with $T = 1.0, \delta = 0.5 \times \varepsilon, N = M$.

$\varepsilon \downarrow$	N=32	N=64	N=128	N=256	N=512	**1024**
Proposed Scheme						
10^{-2}	7.4358e-03	4.6461e-03	2.8525e-03	1.6499e-03	9.2247e-04	4.9675e-04
	0.67847	0.70379	0.78985	0.83880	0.89298	
10^{-3}	7.4345e-03	4.6445e-03	2.8512e-03	1.6494e-03	9.2231e-04	5.06165e-04
	0.67871	0.70395	0.78963	0.83862	0.86564	
10^{-4}	7.4343e-03	4.7302e-03	2.8511e-03	1.6493e-03	9.2229e-04	5.06164e-04
	0.65230	0.73038	0.78966	0.83856	0.86562	
10^{-5}	7.4343e-03	4.7302e-03	2.8511e-03	1.6493e-03	9.2229e-04	5.06164e-04
	0.65230	0.73038	0.78966	0.83856	0.86562	
10^{-6}	7.4343e-03	4.7302e-03	2.8511e-03	1.6493e-03	9.2229e-04	5.06164e-04
	0.65230	0.73038	0.78966	0.83856	0.86562	
10^{-7}	7.4343e-03	4.7302e-03	2.8511e-03	1.6493e-03	9.2229e-04	5.06164e-04
	0.65230	0.73038	0.78966	0.83856	0.86562	
10^{-8}	7.4343e-03	4.7302e-03	2.8511e-03	1.6493e-03	9.2229e-04	5.06164e-04
	0.65230	0.73038	0.78966	0.83856	0.86562	
$E^{N,M}$	7.4358e-03	4.6461e-03	2.8525e-03	1.6499e-03	9.2247e-04	5.06165e-04
$\Gamma^{N,M}$	0.67847	0.70379	0.78985	0.8388	0.86589	
Results in [11]						
10^{-2}	8.25e-03	4.91e-03	2.91e-03	1.68e-03	9.38e-04	5.15e-04
	0.75	0.76	0.79	0.84	0.87	
10^{-3}	8.48e-03	5.11e-03	3.07e-03	1.79e-03	1.02e-03	5.64e-04
	0.73	0.74	0.78	0.81	0.85	
10^{-4}	8.48e-03	5.13e-03	3.09e-03	1.81e-03	1.03e-03	5.74e-04
	0.73	0.73	0.77	0.81	0.84	
10^{-5}	8.48e-03	5.13e-03	3.09e-03	1.81e-03	1.03e-03	5.75e-04
	0.73	0.73	0.77	0.81	0.84	
10^{-6}	8.48e-03	5.13e-03	3.09e-03	1.81e-03	1.03e-03	5.75e-04
	0.73	0.73	0.77	0.81	0.84	
10^{-7}	8.48e-03	5.13e-03	3.09e-03	1.81e-03	1.03e-03	5.75e-04
	0.73	0.73	0.77	0.81	0.84	
10^{-8}	8.48e-03	5.13e-03	3.09e-03	1.81e-03	1.03e-03	5.75e-04
	0.73	0.73	0.77	0.81	0.84	
$E^{N,M}$	8.48e-03	5.13e-03	3.09e-03	1.81e-03	1.03e-03	5.75e-04
$\Gamma^{N,M}$	0.73	0.73	0.77	0.81	0.84	

The calculated $E^{N,M}_{\varepsilon,\delta}$, $E^{N,M}, \Gamma^{N,M}_{\varepsilon,\delta}$ and $\Gamma^{N,M}$ by the scheme in (3.16) for Examples 5.1 and 5.2 are presented in Tables 1 - 4. From tables 1, 2, and 4, one can conclude that the scheme in (3.16) gives more accurate results and rate of convergence than results in [11, 15, 16]. From Tables 1 and 3, one can observe that as $\varepsilon \to 0$ $E^{N,M}_{\varepsilon,\delta}$ decreases as N and M increase, which ratifies the $\varepsilon-$uniform convergence and stability of the proposed numerical scheme.

The influences of the singular perturbation and delay parameters on the boundary layer of the solution for Examples 5.1 and 5.2 are shown in Figures 1 (A) and (B) and 2 (A) and (B). As observed in Figures 1 (A) and (B), when $\varepsilon \to 0$ strong boundary layer is formed near $x = 1$. From Figures 2 (A) and (B), we observe that as the size of the delay parameter increases the thickness of the layer increases.

The physical behavior of the solution of Examples 5.1 and 5.2 for $\varepsilon = 10^{-3}, \delta = 0.8 \times \varepsilon, N = M = 128$ and for different time levels are demonstrated by Figures 3 (A) and (B) respectively. As observed from Figures 3 (A) and (B)

TABLE 2. $E^{N,M}$ and $\Gamma^{N,M}$ for Example 5.1 with $T = 1.0, \delta = 0.9 \times \varepsilon$.

ε	M=60	M=120	M=240	M=480	M=960
$\downarrow$	N=32	N=64	N=128	N=256	N=512
Proposed Scheme					
$E^{N,M}$	5.9248e-03	3.6224e-03	2.1200e-03	1.1970e-03	6.5613e-04
$\Gamma^{N,M}$	0.70982	0.77288	0.82464	0.8674	0.8992
Upwind in [16]					
$E^{N,M}$	1.1359e-02	7.2877e-03	4.4807e-03	2.6516e-03	1.5173e-03
$\Gamma^{N,M}$	0.6403	0.7017	0.7569	0.8054	0.8429
Midpoint upwind in [16]					
$E^{N,M}$	8.3467e-03	5.3894e-03	3.3649e-03	2.0082e-03	1.1571e-03
$\Gamma^{N,M}$	0.6311	0.6796	0.7447	0.7954	0.8341

TABLE 3. $E^{N,M}_{\varepsilon,\delta}$, $E^{N,M}, \Gamma^{N,M}_{\varepsilon,\delta}$ and $\Gamma^{N,M}$ for Example 5.2 with $T = 1.0, \delta = 0.5 \times \varepsilon, N = M$.

$\varepsilon \downarrow$	N=32	N=64	N=128	N=256	N=512	**1024**
2^{-6}	1.3793e-03	7.2750e-04	3.7345e-04	1.8921e-04	9.5228e-05	4.6380e-05
	0.92292	0.96203	0.98093	0.99053	1.0379	
2^{-8}	1.3780e-03	7.2682e-04	3.7310e-04	1.8903e-04	9.5136e-05	4.7622e-05
	0.92291	0.96204	0.98095	0.99055	0.99836	
2^{-10}	1.3777e-03	7.2665e-04	3.7301e-04	1.8899e-04	9.5113e-05	4.7612e-05
	0.92293	0.96205	0.98090	0.99060	0.99832	
2^{-12}	1.3776e-03	7.2660e-04	3.7299e-04	1.8897e-04	9.5107e-05	4.7609e-05
	0.92292	0.96202	0.98098	0.99053	0.99832	
2^{-14}	1.3776e-03	7.2659e-04	3.7299e-04	1.8897e-04	9.5106e-05	4.7608e-05
	0.92294	0.96200	0.98098	0.99055	0.99833	
2^{-16}	1.3776e-03	7.2659e-04	3.7299e-04	1.8897e-04	9.5106e-05	4.7608e-05
	0.92294	0.96200	0.98098	0.99055	0.99833	
2^{-18}	1.3776e-03	7.2659e-04	3.7299e-04	1.8897e-04	9.5106e-05	4.7608e-05
	0.92294	0.96200	0.98098	0.99055	0.99833	
2^{-20}	1.3776e-03	7.2659e-04	3.7299e-04	1.8897e-04	9.5106e-05	4.7608e-05
	0.92294	0.96200	0.98098	0.99055	0.99833	
$E^{N,M}$	1.3793e-03	7.2750e-04	3.7345e-04	1.8921e-04	9.5228e-05	4.7622e-05
$\Gamma^{N,M}$	0.92292	0.96203	0.98093	0.99053	0.99976	

a strong boundary layer is formed near $x = 1$ and as the size of time level increases the thickness of the layer increases. The 3D view of the numerical solution for Examples 5.1 and 5.2 are plotted in Figures 4 (A) and (B) respectively by taking $\varepsilon = 10^{-4}, \delta = 0.5 \times \varepsilon, N = M = 512$, which indicates the existence of the boundary layer near $x = 1$. To depicts the relationship between an $\varepsilon-$uniform $E^{N,M}_{\varepsilon,\delta}$ and the space variable, we have used the Loglog plot in Figures 5 (A) and (B) for Examples 5.1 and 5.2 respectively.

6. CONCLUSIONS

The robust numerical scheme is proposed to solve the singularly perturbed parabolic convection-diffusion equations with a small delay parameter in the spatial variable arising in the modeling of neuronal variability. The scheme is developed, first the term with the shift is approximated by Taylor's series expansion. Then the resulting SPPPDE without shift is solved by using the implicit Euler method and exponentially cubic spline method for the temporal and spatial variable discretization on uniform step sizes. The scheme has shown to be $\varepsilon-$uniformly convergent accuracy of order $O\left((\Delta t) + h^2\right)$. Concisely, the proposed numerical scheme is simple, stable, more accurate, and does not require

TABLE 4. $E_{\varepsilon,\delta}^{N,M}$ for Example 5.2 with $T = 1.0, \delta = 0.5 \times \varepsilon$.

ε ↓	M=2048 N=32	N=64	N=128	N=256
Proposed Scheme				
2^{-6}	3.5200e-03	2.0942e-03	1.2371e-03	7.4919e-04
2^{-10}	3.5148e-03	2.0912e-03	1.2355e-03	7.4837e-04
2^{-14}	3.5144e-03	2.0910e-03	1.2354e-03	7.4832e-04
2^{-18}	3.5144e-03	2.0910e-03	1.2354e-03	7.4832e-04
2^{-20}	3.5144e-03	2.0910e-03	1.2354e-03	7.4832e-04
Modified upwind method in [15]				
2^{-6}	1.19749e-02	9.50610e-03	6.56708e-03	4.38502e-03
2^{-10}	1.19643e-02	9.50508e-03	6.56490e-03	4.38488e-03
2^{-14}	1.19637e-02	9.50502e-03	6.56476e-03	4.38487e-03
2^{-18}	1.19636e-02	9.50501e-03	6.56475e-03	4.38487e-03
2^{-20}	1.19636e-02	9.50501e-03	6.56475e-03	4.38487e-03
Upwind method in [15]				
2^{-6}	1.29843e-02	9.85791e-03	6.76565e-03	4.47863e-03
2^{-10}	1.29892e-02	9.86467e-03	6.76915e-03	4.48178e-03
2^{-14}	1.29885-02	9.86460e-03	6.76901e-03	4.48177e-03
2^{-18}	1.29885e-02	9.86459e-03	6.76900e-03	4.48176e-03
2^{-20}	1.29885e-02	9.86459e-03	6.76900e-03	4.48176e-03

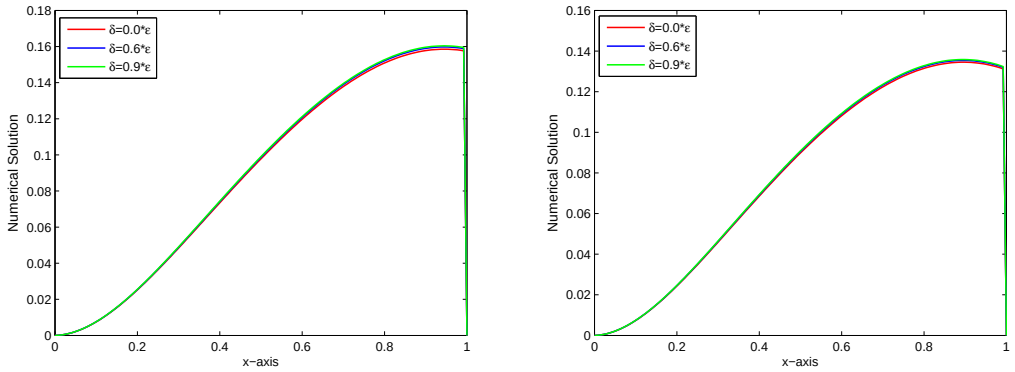

(A) Example 5.1 (B) Example 5.2

FIGURE 2. Effect of delay on the solution behavior for $T = 1, \varepsilon = 2^{-4}$, and $N = M = 128$.

a priori information about the location and width of the boundary layer. The scheme can also be extendable for solving higher order families of differential-difference problems. **However, the limitation of the scheme is it's being restricted on small shift.**

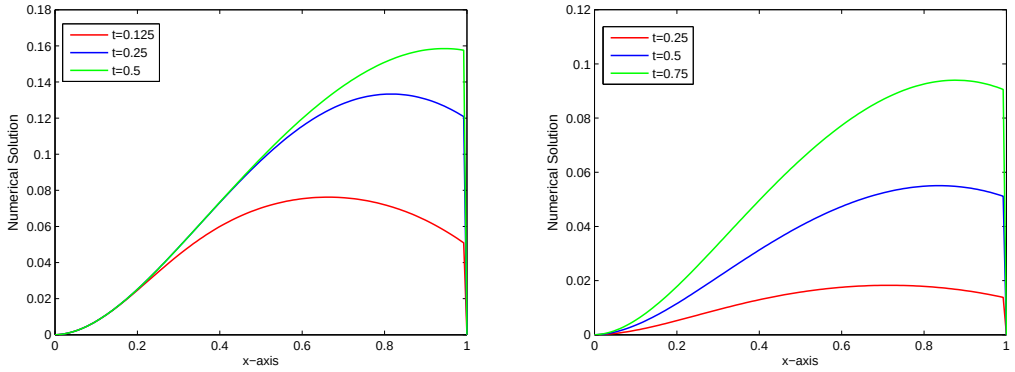

(A) Example 5.1 (B) Example 5.2

FIGURE 3. Effect of time t level on the solution behavior for $\varepsilon = 10^{-3}, \delta = 0.8 \times \varepsilon, N = M = 128$.

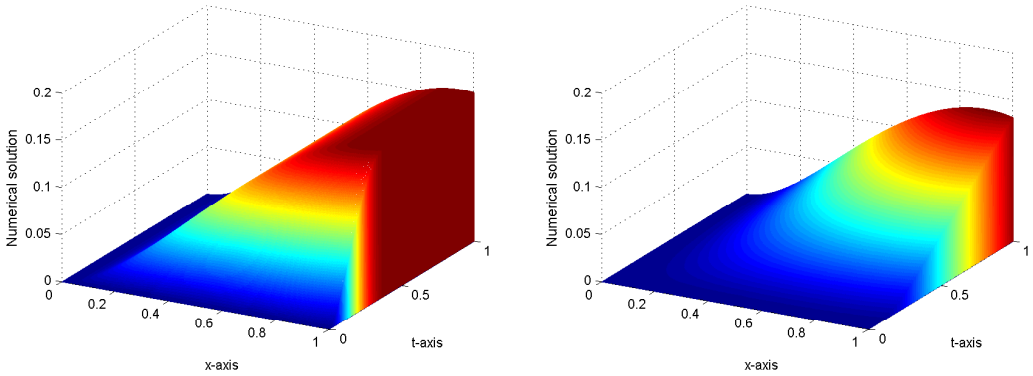

(A) Example 5.1 (B) Example 5.2

FIGURE 4. 3D view of numerical solution profiles for $T = 1.0$,$\varepsilon = 10^{-4}, \delta = 0.5\times\varepsilon$, and $N = M = 512$.

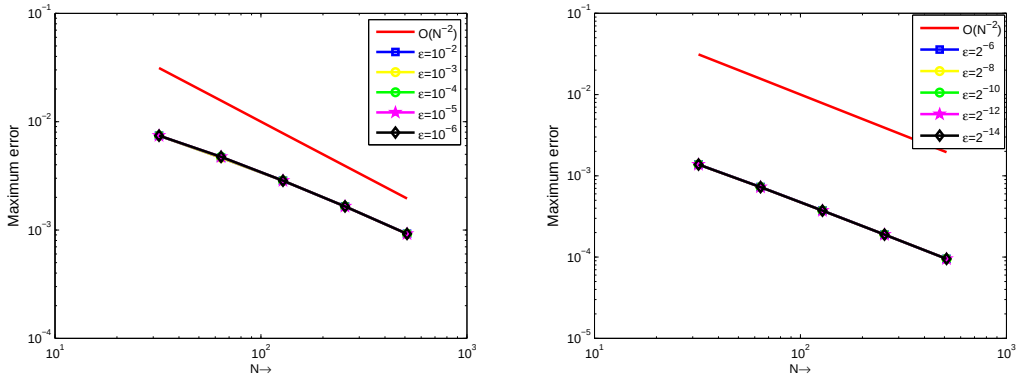

(A) Example 5.1 (B) Example 5.2

FIGURE 5. Loglog plot of the maximum pointwise errors.

References

[1] N. S. Bakhvalov, *Towards optimization of methods for solving boundary value problems in the presence of a boundary layer*, Zh. Vychsl. Mat. Fiz., *9* (1969),841–859.

[2] K. Bansal, P. Rai, and K. K. Sharma, *Numerical treatment for the class of time dependent singularly perturbed parabolic problems with general shift arguments*, Differential Equations and Dynamical Systems, *25*(2) (2017), 1–20.

[3] K. Bansal and K. K. Sharma, *Parameter uniform numerical scheme for time dependent singularly perturbed convection-diffusion-reaction problems with general shift arguments*, Numer Algor., *75*(1) (2017),113–145.

[4] S. Boulaaras, *Some new properties of asynchronous algorithms of theta scheme combined with finite elements methods for an evolutionary implicit 2-sided obstacle problem*, Mathematical Methods in the Applied Sciences, *40*(18) (2017), 7231–7239.

[5] S. Boulaaras and M. Haiour , $L^{\infty-}$asymptotic behavior for a finite element approximation in parabolic quasi-variational inequalities related to impulse control problem, Applied Mathematics and Computation, *217*(14) (2011), 6443–6450.

[6] S. Boulaaras and M. Haiour, *The finite element approximation of evolutionary Hamilton–Jacobi–Bellman equations with nonlinear source terms*, Indagationes Mathematicae, *24*(1) (2013), 161–173.

[7] S. Boulaaras, M. Haiour, and M. E. Bencheick ,*Error estimates of discontinuous Galerkin methods with theta time discretization scheme for an evolutionary HJB equations*, Mathematical Methods in the Applied Sciences, *40*(12) (2017), 4310–4319.

[8] S. Boulaaras, M. Haiour, and M. E. Bencheick, *A new error estimate on uniform norm of a parabolic variational inequality with nonlinear source terms via the subsolution concepts*, Journal of Inequalities and Applications, *2020*(1) (2020), 1–18

[9] T. A. Bullo, G. F. Duressa, and G. Degla, *Accelerated fitted operator finite difference method for singularly perturbed parabolic reaction-diffusion problems*, Computational Methods for Differential Equations, *9*(3) (2021), 886-898.

[10] I. T. Daba and G. F. Duressa, *Extended cubic B-spline collocation method for singularly perturbed parabolic differential-difference equation arising in computational neuroscience*, International Journal for Numerical Methods in Biomedical Engineering, *37*(2) (2021), e3418.

[11] D. Kumar, *An implicit scheme for singularly perturbed parabolic problem with retarded terms arising in computational neuroscience*, Numerical methods Partial Differential Eq., *34*(6) (2018),1933-1952.

[12] O. A. Ladyzhenskaia, V. A. Solonnikov, and N. N. Ural'tseva, *Linear and quasi-linear equations of parabolic type*, American Mathematical Soc., (1968), 23.

[13] M. Musila and P. Lansky, *Generalized Stein's model for anatomically complex neurons*, BioSystems, *25*(1991),179-191.

[14] R. E. O'Malley, *Introduction to singular perturbations*, North-Holland Series in Applied Mathematics & Mechanics, 1974.

[15] V. Ramesh and B. Priyanga, *Higher order uniformly convergent numerical algorithm for time-dependent singularly perturbed differential-difference equations*, Differential Equations and Dynamical Systems, *29*(1) (2021), 1–25.

[16] V. P. Ramesh and M. K. Kadalbajoo, *Upwind and midpoint difference methods for time dependent differential difference equations with layer behavior,* Applied Mathematics and Computational, *202*(2) (2008), 453–471.

[17] A. S. V. Ravi Kanth and P. M. M. Kumar,*Numerical treatment for a singularly perturbed convection delayed dominated diffusion equation via tension splines*, International Journal of Pure and Applied Mathematics, *113*(6) (2017), 110–118.

[18] H. G. Roos, M. Stynes, and L. R. Tobiska, *Robust numerical methods for singularly perturbed differential equations: convection-diffusion-reaction and flow problems*, Springer Science and Business Media, (2008), 24.

[19] G. I. Shishkin, *A difference scheme for a singularly perturbed parabolic equation with a discontinuous boundary condition*, Zh. Vychisl. Mat. Mat. Fiz., *28*(6) (1988), 1679–1692.

[20] R. B. Stein, *Some models of neuronal variability*, Biophysical journal, *7*(1) (1967), 37–68.

[21] H. Tian, *The exponential asymptotic stability of singularly perturbed delay differential equations with a bounded layer.*, Journal of Mathematical Analysis and Applications, *270*(1) (2002), 143–149.
[22] M. M. Woldaregay and G. F. Duressa, *Parameter uniform numerical method for singularly perturbed parabolic differential difference equations*, Journal of the Nigerian Mathematical Society, *38*(2) (2019), 223–245.
[23] H. Zadvan and J. Rashidinia, Development of non polynomial spline and New B-spline with application to solution of Klein-Gordon equation, Computational Methods for Differential Equations, *8*(4) (2020),794–814.
[24] W. K. Zahra and A. M. El Mhlawy,*Numerical solution of two-parameter singularly perturbed boundary value problems via exponential spline*, Journal of King Saud University Science, *25*(3) (2013), 201–208.